Journal of Archaeological Science 186 (2026) 106473

Contents lists available at ScienceDirect

Journal of Archaeological Science

journal homepage: www.elsevier.com/locate/jas

Bioarchaeological signatures during the Plague of Justinian (541–750 CE) in Jerash (ancient Gerasa), Jordan

Karen Hendrix [a], Swamy R. Adapa [b], Robert H. Tykot [c], Gregory O'Corry-Crowe [d], Andrea Vianello [c], Gloria C. Ferreira [e,f], Michael Decker [g], Rays H.Y. Jiang [b,*]

[a] Discipline of Archaeology, School of Humanities, University of Sydney, Australia
[b] USF Genomics, Global Health Infectious Disease Research Center (GHIDR), Global Health, College of Public Health, University of South Florida, Tampa, FL, USA
[c] Department of Anthropology, University of South Florida, Tampa, FL, USA
[d] Harbor Branch Oceanographic Institute, Florida Atlantic University, Fort Pierce, FL, USA
[e] Department of Molecular Medicine, Morsani College of Medicine, University of South Florida, Tampa, 33612, FL, USA
[f] Department of Chemistry, College of Arts and Sciences, University of South Florida, Tampa, 33620, FL, USA
[g] Department of History, University of South Florida, Tampa, FL, USA

ARTICLE INFO

Keywords:
First Pandemic Jerash
Roman-Byzantine archaeology
Stable isotopes
Ancient DNA
Mass grave
Mitochondrial haplogroups

ABSTRACT

Jerash (ancient Gerasa, in modern day Jordan) reached its demographic peak in the 3rd century CE with a population of roughly 25,000, but by the end of the 6th century this had declined to about 10,000, setting the stage for the urban vulnerabilities examined in this study. The W2 and W3 chambers of the Jerash hippodrome contain a densely layered mass burial of ~230 individuals dating to the mid-6th to early 7th century AD. Through archaeological documentation, stable isotope analysis, and ancient DNA study, we present the first biomolecularly confirmed mass grave associated with the First Pandemic (Justinianic Plague) in the Eastern Mediterranean. The taphonomic pattern, rapid, high-density deposition with minimal funerary structuring, closely parallels catastrophic plague pits of the later medieval period, making Jerash a uniquely well-preserved example from Late Antiquity.

Stable carbon and nitrogen isotope values from human bone collagen indicate diets dominated by C3 resources typical of the region. In contrast, oxygen isotope values from tooth enamel display a markedly wider range than those documented in long-term residential populations at Tell Dothan, Pella, or Faynan in the Levant. Although oxygen isotopes cannot specify geographic origin, the magnitude of variation, arising within a burial event deposited over only days or weeks, suggests that the individuals interred in the Jerash mass grave grew up in diverse childhood water ecologies. We interpret this pattern conservatively as evidence of heterogeneous lived experiences among the victims during the crisis.

Ancient DNA analysis has recently identified a single, uniform strain of *Yersinia pestis*, confirming a synchronous epidemic event. In this study, mitochondrial haplogroups H13 and L3e were detected among the victims and fall within the expected maternal diversity of the Byzantine Levant.

Taken together, the archaeological, isotopic, and genetic results establish Jerash as the earliest securely identified catastrophic plague burial in the Near East. The First Pandemic concentrated a potentially socially and geographically heterogeneous population into a single mortuary event, providing a rare empirical window into mobility, urban life, and vulnerability in Late Antiquity. Jerash thus offers a critical anchor point for reconstructing the demographic and epidemiological landscape of the early medieval Mediterranean.

1. Introduction

The First Pandemic (541–750 CE), known historically as the Plague of Justinian, marked one of the earliest recorded instances of large-scale infectious disease outbreaks in the Old World (Eisenberg and Mordechai, 2020; Sarris, 2002, 2022). While its devastating effects on urban centers across the Eastern Roman (Byzantine) Empire have been documented in historical texts (Sarris, 2002, 2022), the lived experiences of affected

* Corresponding author.
E-mail address: Jiang2@usf.edu (R.H.Y. Jiang).

https://doi.org/10.1016/j.jas.2026.106473
Received 3 September 2025; Received in revised form 14 December 2025; Accepted 3 January 2026
Available online 13 January 2026

communities remain largely unknown. The lack of temporal control for many cemeteries makes it difficult to identify specific burials containing individuals who died during a plague outbreak. Direct confirmation of the presence of a disease outbreak can be achieved through pathogen aDNA analysis.

Jerash, located in present-day Jordan, was a thriving Late Byzantine provincial city during the 6thand early 7th centuries CE. As part of the Decapolis region (Kennedy, 2013) (Fig. 1A), it served as a trade, religious, and administrative hub connected to major networks across the Eastern Mediterranean, including Egypt, Syria, and Anatolia. This connectivity, while contributing to Jerash's economic and cultural vitality, may also have rendered it particularly vulnerable to the rapid spread of infectious disease.

Excavations in the southwest quarter of Jerash uncovered a densely packed mass grave, unprecedented in its mortuary context (Ostrasz, 1991). This mass grave, with no evidence of violence or extended funerary treatment (Hendrix, 1995, 1998), strongly suggests a mass mortality event, likely a localized impact of the First Pandemic.

In this study, we integrate archaeological observations with stable isotope analysis and mitochondrial DNA (mtDNA) to investigate the demographic composition of the individuals buried in the Jerash mass grave. Our goal is to assess what this assemblage reveals about the people who died during the First Pandemic and how their biological signatures correspond to the archaeological and historical context of crisis-driven interment. By combining taphonomy, isotopic data, and maternal lineage information, we characterize the population represented in the grave and clarify the social and environmental conditions surrounding mortality in a provincial Byzantine city. This multidisciplinary approach provides a framework for understanding community structure, vulnerability, and lived experience during the pandemic in Late Antiquity.

2. Historical background: Jerash at the convergence of pandemic and regional change

From the 4th to the early 7th centuries CE, Jerash stood as a prominent city within the province of *Arabia*, part of the Roman/Byzantine Empires. Located in the highlands of modern central northern Jordan, Jerash was situated at the nexus of inland trade and communication routes that connected the cities of the Decapolis to the Jordan Valley and the broader Mediterranean world (Kennedy, 2013) (Fig. 1A.) These arterial routes linked Jerash with regional centers such as Pella (modern Tabaqat Fahl), Scythopolis (modern Beth Shan), Caesarea Maritima, and Damascus, thereby facilitating a vibrant exchange of goods, people, and ideas across Syria, Palestine, and Arabia Petraea.

By the early Byzantine period (4th and 5th centuries CE) Jerash had already become a flourishing urban center known for its monumental architecture, including a Hippodrome, colonnaded streets, temples, theaters, and baths. When Constantine I shifted his administration center to Constantinople in 324CE, it underlined the changes occurring within the eastern Mediterranean world, predominantly the rise of Christianity (Watson, 2008). Changes in cities occurred with public buildings, temples and hippodromes falling into disuse or being repurposed for other activities, such as industrial workshops in Jerash (Kehrberg and Ostrasz, 1997). Flourishing civic life in the 4th to 6th century CE was evidenced by multiple church constructions, during or shortly after the reign of the Emperor Justinian (527–565 CE) (Lichtenberger et al., 2021). The city's integration into long-distance trade networks and its role as a religious and administrative hub made it a nodal point in the Byzantine provincial system (Watson, 2008).

The urban setting would have increased Jerash's vulnerability during the First Pandemic (541–750 CE). Although Jerash is not mentioned in extant plague chronicles, the epidemic is extensively documented in nearby cities. Procopius describes the plague's catastrophic arrival in Constantinople in 542 CE, while John of Ephesus and Evagrius Scholasticus provide detailed accounts of successive outbreaks in Antioch, Jerusalem, Gaza, and Alexandria through the late 6th and early 7th centuries (Bystrický, 2023; Lichtenberger et al., 2021). Given Jerash's position within these overlapping spheres of travel and communication, it is highly likely that the plague reached the city, even if this escaped specific textual mention.

In line with patterns observed elsewhere, Jerash experienced economic and demographic decline in the late 6th and 7th centuries, a period marked by reduced monumental construction, abandonment of urban structures, and shifts in land use (Kehrberg, 2009; Kennedy, 2007). Scholars have supported multifactorial events, including climate change, epidemics, earthquakes and droughts as significant factors in the decline of the Byzantine Empire (Al-Shorman, 2022; McDonald, 2024). Such transformations parallel accounts of social disruption and administration collapse caused by the plague from across the empire. The reuse of civic architecture for non-traditional purposes, specifically interments within a former hippodrome, is exceptional among archaeological cases from the First Pandemic period. While scholars like Little (2007) document how plague outbreaks overwhelmed city burial systems, no comparable examples are recorded in urban centers like Constantinople. Jerash thus represents a rare and illuminating example of adaptive funerary practices under pandemic stress.

Jerash's Roman historical position as a regional administrative center, linked to wider Jordan Valley trade routes, placed it within a landscape of declining economic and political fortunes in the sixth–seventh centuries of turbulent times (Rapp, 2023). As the city entered a period of contraction and declining civic capacity, its connections to surrounding rural and monastic hinterlands likely continued to shape the composition of its population. The isotopic and genetic data from the mass grave provide an unusual opportunity to examine this broader regional context and to assess how the city's late antique trajectory may be reflected in the individuals buried during the First Pandemic.

2.1. Sample selection and materials

The skeletal collection was housed in the storage facility at Jerash under the authority of the Department of Antiquities of Jordan. The samples selected for this study were obtained during the initial analysis in 1995/1998, with a view to undertaking further investigations. Since the initial osteological examination of the mass grave in the 1990s, further access to the collection has not been possible.

All the sampled teeth are permanent, loose (not in occlusion) molars with well-preserved enamel. Thirty-seven adult mandibular and maxillae molars (1st, 2nd and 3rd molars) were chosen for examination based on their overall completeness: lack of caries and other dental diseases. To obtain samples from different individuals the teeth were selected from different areas of the chambers. Two adult ribs were also selected, which represented two different individuals. As the samples came from commingled deposits and the teeth were not associated with alveolar bone, age and sex were not estimated and it is acknowledged that this limits the potential for extensive demographic profiling.

Of the 37 samples provided for examination 8 teeth were suitable for aDNA and mtDNA studies. For both stable isotope and ancient DNA analysis, 11 samples, consisting of 10 teeth and 1 rib were considered suitable for analysis (Table 1.)

2.2. aDNA extraction and analysis

Ancient DNA (aDNA) was extracted and analyzed from human teeth selected from the Jerash mortuary assemblage as previously described (Adapa et al., 2025). Briefly, the samples were chosen based on preservation quality and absence of surface contamination. To reduce exogenous contamination, each tooth underwent rigorous surface decontamination using a mild bleach wash followed by mechanical abrasion. All aDNA work was conducted in a dedicated, certified cleanroom facility, which had not previously processed human or

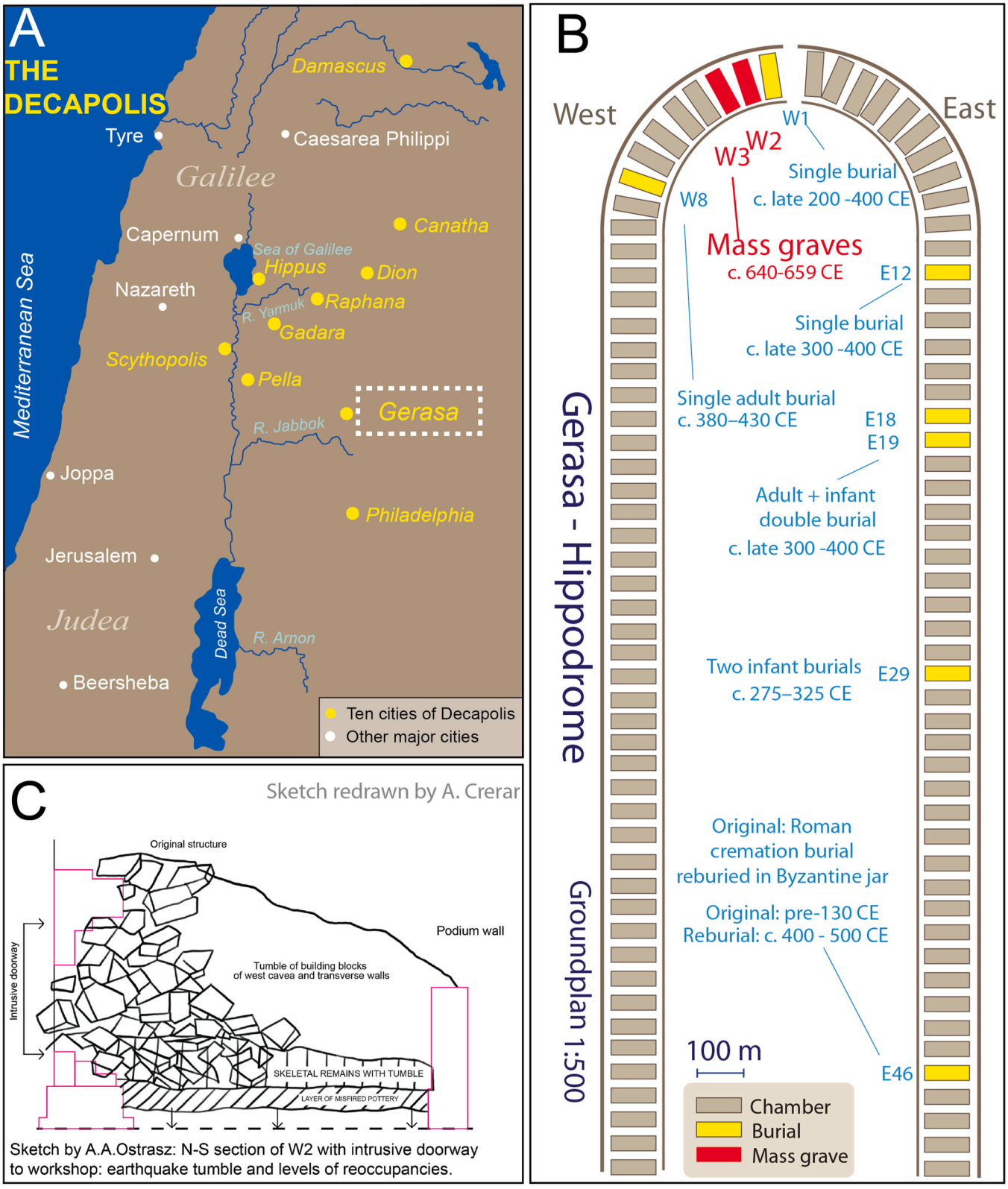

Fig. 1. Location of Jerash and section sketch of Mass Grave W2. A. Map of the ten cities of the Decapolis, with Jerash (Gerasa) highlighted by a dotted-line box. Base map adapted from Nichalp, CC BY-SA 2.5. **B.** Ground plan of the Jerash hippodrome showing the distribution of burials, adapted from the original plan by Ostrasz with burial locations as published by Kehrberg and Ostrasz (2017). The interments span the full sequence of activity at the site, from a Roman cremation burial in a jar, to Byzantine-period reburials, workshop-associated single and double inhumations, and finally the two mid-7th-century mass graves. Mass Graves W2 and W3 represent the latest burials excavated within the hippodrome. **C.** North–south section sketch of Mass Grave W2. Original drawing by Ostrasz, redrawn by A. Crerar. Pink shaded areas denote structural elements of the hippodrome. Human remains lie compacted between layers of misfired pottery waste and blocks from earthquake collapse, indicating rapid interment within an abandoned industrial context. (For interpretation of the references to colour in this figure legend, the reader is referred to the Web version of this article.)

Table 1
Overview of individuals analyzed for ancient DNA and stable isotopes from the Jerash mass grave.

Grave Chamber	Individual ID	aDNA Material Analyzed	aDNA genetic data	Isotope Material Analyzed
W2	**W2-100**	–		W2-100 (LM2)
W2	**W2-110**	W2-110(a) – LM3	*Y. pestis*	W2-110(c) – LM2
W2	**W2-115**	–		W2-115 – LM2
W2	**W2-118**	W2-118(h) – LM2; W2-118 (e) – RM1	*Y. pestis*	W2-118(a) – RM2
W2	**W2-126**	–		W2-126 – M2
W2	**W2-127**	–		W2-127 – RM2
W2	**W2-130**	W2-130(e) – RM2; W2-130 (d) – LM2	*Y. pestis and Human mt Haplotype*	W2-130(a) – LM2
W3	**W3-69**	–		W3-69(e) – RM2
W3	**W3-75**	–		W3-75(a) – RM3
W3	**W3-77**	–		W3-77 – incisor
W2	**W2-131**	W2-131 – M3	*Y. pestis and Human mt Haplotype*	–
W2	**W2-122**	W2-122(c) – RM2; W2-122 (d) – LM3	*Y. pestis*	–
W2	**Unidentified**	–		Unidentified

LM/RM = left or right molar; number indicates tooth position (*e.g.*, LM2 = left second molar).
aDNA samples correspond to dentin/root used for ancient DNA extraction; isotope samples correspond to enamel used for $\delta^{13}C$, $\delta^{15}N$, and $\delta^{18}O$ measurements.

pathogen samples. This facility followed strict protocols for aDNA handling, including the use of personal protective equipment, laminar flow hoods, and negative controls throughout the workflow.

Approximately 0.5 g of tooth powder were extracted per sample using a sterile drill. Powdered samples were subjected to decalcification in 0.5 M EDTA (pH 8.0) prior to DNA extraction, following established protocols optimized for ancient samples library preparation employed a modified protocol tailored to degraded DNA, including enzymatic end-repair, adapter ligation, and indexing with unique barcodes. Library amplification was limited to minimize bias from damaged fragments. Sequencing was conducted using Illumina paired-end technology to ensure high-resolution genomic coverage.

All ancient DNA extractions and library preparations were accompanied by multiple extraction blanks and library blanks processed in parallel with the archaeological samples. These controls were carried through all downstream steps, including indexing, amplification, and sequencing. Negative controls yielded no detectable reads mapping to human or *Yersinia pestis*, confirming the absence of laboratory contamination. Only sequencing runs in which blank controls were clean were used for downstream analyses.

Ancient DNA libraries were prepared using both uracil–DNA glycosylase (UDG–treated) and non-UDG protocols to enable high-confidence molecular authentication and downstream genomic analyses. UDG-treated libraries reduce cytosine deamination and provide cleaner consensus sequences for mitochondrial and nuclear targets, while non-UDG libraries retain characteristic terminal damage patterns essential for verifying ancient DNA authenticity. All libraries were sequenced on Illumina NextSeq platforms in paired-end mode, generating high-complexity datasets suitable for both endogenous human DNA recovery and pathogen screening. Mitochondrial DNA was recovered from all individuals. Data were deposited in the NCBI Sequence Read Archive, where raw output is reported as "spots," each corresponding to a paired-end sequencing event.

Authentication of aDNA was confirmed using multiple lines of evidence. The sequenced fragments were predominantly short (~100 base pairs), consistent with expected degradation patterns in ancient samples. Damage patterns characteristic of aDNA, such as cytosine deamination at fragment termini, were also observed. Additionally, taxonomic and phylogenetic analyses of both microbial and human sequences aligned with ancient origin, supporting the authenticity of the recovered material. Mitochondrial DNA (mtDNA) reads were successfully retrieved from two individuals, providing further confirmation and enabling assessment of maternal lineages.

2.3. Stable isotope analysis ($\delta^{13}C$, $\delta^{15}N$, $\delta^{18}O$)

Stable isotope analysis was conducted on the samples of dentition and bone to infer dietary practices and childhood geographic origins. The analytical approach closely followed protocols previously established for archaeological samples (Tykot, 2020). For $\delta^{13}C$ and $\delta^{15}N$ measurements, collagen was extracted from dentin and rib samples using a well-established method removing the mineral apatite (Tykot, 2020). Bone collagen was extracted by demineralizing whole bone using 2 % hydrochloric acid for 72 h, dissolving base-soluble contaminants using 0.1 M sodium hydroxide (24 h before and after demineralization), and separating residual lipids with a mixture of methanol, chloroform and water for 24 h. Collagen pseudomorphs were analyzed at the USF Paleo Stable Isotope Laboratory for carbon and nitrogen isotopes using a CHN analyzed coupled with a Finnigan MAT Delta + XL continuous flow SIRA with Carlo-Erba NA2500 EA. Along with visual analyses and data from the sample preparation including collagen yield, C:N ratios of the analyzed gases of 2.9–3.6 were determined to be reliability of the isotope results.

To assess $\delta^{18}O$ and additional $\delta^{13}C$ values from early life, enamel samples were taken from second molars. Enamel apatite was pretreated for 24 h each with 2 % sodium hypochlorite to remove organic contaminants, followed by 1 M buffered acetic acid to remove secondary carbonates (Tykot, 2020), Isotope ratios were measured using a ThermoFisher MAT253 isotope ratio mass spectrometer coupled to a GasBench-II + continuous-flow interface at the University of South Florida Paleo Laboratory. Calibration was performed using internationally recognized standards as well as compared with other laboratories.

These methods were used to examine dietary protein sources (via $\delta^{13}C$ and $\delta^{15}N$ from collagen) and early geographic origin (via $\delta^{18}O$ and $\delta^{13}C$ from enamel), to provide a high-resolution view of population diversity and mobility at Jerash during the First Pandemic.

3. Results

3.1. Archaeological excavation of W2 and W3 in the hippodrome

The hippodrome was constructed between mid 2nd century to 209-212 CE and later abandoned for racing within one hundred years due to disintegration of the masonry, a direct result of poor foundations (Kehrberg and Ostrasz, 1997). Thereafter, it transitioned into an industrial zone, before falling into disuse altogether by the late 6th century (Ostrasz, 1993). The final occupational layer, an abrupt sealing of misfired pottery, signals not only economic cessation but also a shift in how this monumental space was perceived and used. It is atop this abandoned industrial floor that one of the largest mass graves in the Levant was later deposited, its skeletal assemblage entangled within the collapsed architectural debris (Little, 2007; Kehrberg, 2009, 2016). (Fig. 1C)

The excavation, restoration and utilization of the hippodrome have been widely published by the Polish/Jordanian excavation team over several decades (Kehrberg, 2009, 2016; Kehrberg and Ostrasz, 1994, 1997, 2017; Ostrasz, 1989, 1991, 1993; Ostrasz and Kehrberg-Ostrasz, 2020).

The excavation of several *cavea* chambers (a storage space below the

seating) of the hippodrome revealed several incidences of graves both within the *cavea* chambers and in the grounds outside. Most of these are described as simple burials (except *cavea* chambers W2 and W3) and pertain to the reuse of the hippodrome for burial and industrial activities (Kehrberg and Ostrasz, 2017) (Fig. 1B). The use of the hippodrome as a place for light industrial activity and ceramic production included ceramic workshops dating from the Late Roman period that continued into the Early Byzantine period (mid-4th century CE). A compact layer of misfired and unfired Late Byzantine (the second half of the 6th century CE) pottery, including fragments of 'Jerash Bowls', sealed these installations. The entire building was abandoned around the latter part of the 6th century CE or beginning of the 7th century CE.

By the end of the Byzantine era (636–640 CE) the potter's community had abandoned the hippodrome site, and all activity in W2 and W3 *cavea* chambers ceased before the bodies were interred (Kehrberg and Ostrasz, 1997, 2017).

The 1991–1993 excavation of the W2 and W3 *cavea* chambers in the hippodrome revealed a large mass grave holding hundreds of human skeletal remains, crushed by tumbled stone blocks from the vault of the chamber (Kehrberg and Ostrasz, 2017) (Fig. 1C).This mass grave lay above disused workshop installations, and a compact layer of discarded misfired and unfired pottery and lamps, from extensive pottery production of the late Byzantine period (Kehrberg, 2009).

The chambers were excavated in horizontal levels, each equivalent to the height of a course of blocks that made up the walls of each chamber. Within those levels discrete clusters of commingled bones were allocated a "lot" number.

3.2. Archaeological dating of the Jerash Mass burial

The chronology of the W2–W3 mass burial is constrained by a converging set of ceramic, numismatic, architectural, and historical indicators (Table 2). Stratigraphically, the human remains overlie extensive pottery dumps associated with the final phase of activity in the hippodrome workshops) (Kehrberg and Ostrasz, 2017; Kehrberg, 2009). These deposits include large quantities of unfired and misfired ceramics, indicating abrupt workshop abandonment shortly before the chambers were repurposed as a mass burial space.

Ceramic evidence refines the chronology. The assemblage includes characteristic "Jerash bowls," a locally produced fineware tradition spanning approximately the first quarter of the sixth through the mid-seventh century CE, with peak production around 575–600 CE. The presence of unfired vessels within the burial fill indicates that the potters' workshops were abandoned abruptly, plausibly around 640 CE, shortly before or during the mortuary episode.

A gold tremissis recovered from *Lot 130* in chamber W2 provides a critical terminus post quem. The coin was minted during the reign of either Constans II (641–668 CE) or Constantine IV (668–685 CE)[1]; although surface damage prevents definitive attribution, numismatic assessment favors Constans II (Kehrberg and Ostrasz, 2017). The coin was found in direct association with beads and skeletal remains at the lowest level of the mass grave (Level 5 in W2). A molar recovered from this context (sample W2-130(d)) was included in the present analyses. While the tooth was not embedded in an articulated maxilla, its spatial association strongly suggests derivation from this robust individual.[2]

Table 2
Integrated archaeological, numismatic, and historical chronology of the Jerash W2–W3 mass burial.

Approximate Date	Event [a,b,c,d]	Primary Evidence	Interpretive Significance
ca. 575–600 CE	Peak production of *Jerash bowls*	Ceramic typology; workshop assemblages	Establishes late 6th-century industrial activity immediately preceding the burial episode
ca. 640 CE	Abandonment of pottery workshops; accumulation of misfired ceramics	Unfired vessels and workshop debris stratigraphically associated with human remains	Indicates abrupt cessation of production consistent with crisis disruption
641–668 CE	Reign of Constans II (probable coin attribution)	Gold tremissis recovered from W2 chamber	Provides a *terminus post quem* for burial deposition and subsequent chamber collapse
ca. 640–659 CE	Deposition of the W2–W3 mass burial	Dense, rapidly deposited human remains above workshop debris and below collapse layers	Indicates acute mortality event requiring extraordinary burial response
659 CE	Earthquake collapse sealing the chambers	Structural damage consistent with regionally attested seismic event	Provides a *terminus ante quem* for the burial assemblage

[a] Numismatic attribution to Constans II remains tentative due to surface damage; however, the coin securely establishes a seventh-century *terminus post quem.*

[b] The ceramic horizon spans ca. 525–650 CE, with peak production between 575 and 600 CE; unfired ceramics indicate abandonment rather than gradual decline.

[c] The earthquake is archaeologically documented elsewhere in the hippodrome complex and regionally dated to 659 CE, sealing the W2–W3 chambers and preserving the burial context.

[d] This integrated framework aligns most parsimoniously with early seventh-century plague episodes, particularly the Plague of Amwas (638–639 CE), though the table itself reflects archaeological dating independent of historical attribution.

Following deposition of the bodies, an earthquake caused collapse of the cavea seating, sealing the skeletal assemblage beneath architectural debris. Earthquake damage is well documented across Jordan during Late Antiquity and the early Islamic period, both archaeologically and historically (Watson, 2008; Al-Shorman, 2022). At the hippodrome, Ostrasz (1991) identified structural destruction consistent with an earthquake dated to 659 CE, which affected large portions of the seating complex and is interpreted as the event that sealed the W2–W3 deposits. A later catastrophic earthquake in 747 CE destroyed the hippodrome entirely but postdates the burial context.

This archaeological horizon aligns closely with the historical epidemiology of the region. Earlier sixth-century plague waves reported in historical sources for 592 and 599/600 CE are geographically plausible but chronologically remote relative to the depositional context at Jerash (Conrad, 1981, 1994). More compelling are early seventh-century outbreaks recorded by Near Eastern chroniclers. Agapios describes epidemic episodes in Syria and Phoenicia between 634 and 665 CE, some following earthquakes, while Michael the Syrian records the plague of Shiraway in 627 CE, said to have claimed "many myriads" of lives (Russell, 1968; Haldon and Stathakopoulos, 2018; Brock, 1976).

Most relevant, however, is the Plague of ʿAmwās (638–639 CE), a major pandemic episode that affected Syria and Palestine during the early Islamic conquests (Dols, 1974). Given the firm terminus post quem provided by the coinage, the ceramic production horizon, evidence for abrupt workshop abandonment, and the historically documented cluster of epidemics in the 620s–630s, the Plague of ʿAmwās could represent the

[1] If the coin is dated to Constans II it would potentially offer a *terminus post quem* for the mass grave at 641CE. If it is dated to Constantine IV then the coin may have shifted from the surface during the collapse of *cavea* chamber, having laid on the surface for an undetermined amount of time.

[2] W2-Lot 130 -a deposit at the bottom of the chamber, had an MNI of 8 individuals, 3 Adults – 2 male and 1 female, 3 subadults and 2 children. One of the males (W2-130 #1) displayed robust post cranial elements. Considering the size of the tooth in the study W2-130(d) there is a strong possibility this tooth belonged to this individual.

most parsimonious chronological and epidemiological match for the Jerash mass burial.

3.3. Archaeological indications of urban mortality in Jerash

The mass grave uncovered beneath collapsed seating of the Jerash hippodrome stands as one of the most evocative urban mortality assemblages from the Eastern Mediterranean during Late Antiquity. Previous accounts described the site primarily in terms of architectural reuse or local disaster contexts (Kennedy, 2013; Kehrberg and Ostrasz, 2017). Our interdisciplinary analyses, genetic, isotopic, and archaeological, invite a re-evaluation of its broader significance within the landscape of pandemic-era urbanism.

According to the excavation report (Kehrberg and Ostrasz, 2017; Ostrasz, 1991) there was no orderly pattern to the position of the bodies, apart from several individuals who appeared to have been carefully placed indicating that these individuals were amongst those that died early in the pandemic. Subsequent burials lying immediately above were disarticulated. The disarticulation of these individuals is likely multifactorial, including the communities need to quickly bury its dead, post-mortem activity such as decomposition of the skeletons and the impact of the large block of stones tumbling into the *cavea* chamber from a later earthquake. Overall, the excavators consider that most of these individuals were deposited in the chambers within a short time span. (Kehrberg and Ostrasz, 1994).

Preliminary osteological examination of the skeletal remains was undertaken in 1995 and 1998 and this investigation indicated the presence of 150 adults and 80 sub adults (neonates, infants and children). Each "lot" was analyzed to determine a Minimum Number of Individuals (MNI). Demographic profiles were determined by standards recommended by Buikstra and Ubelaker (Buikstra and Ubelaker, 1994), where possible for identifiable skeletal elements. A final MNI was given once the analysis of all "lots" was undertaken from both chambers.

Paleopathological examination indicated joint, metabolic, and infectious diseases and several healed fractures but these were within the bounds of what would be expected within this small sample (Hendrix, 1995). The fracturing of the bones is considered to have occurred when the bones were dry and having lost their collagen (Hendrix, 1995). This factor precludes the possibility that the earthquake event occurred shortly after the deposition of the bodies, with more than a decade or more between the two events.

It is not possible to be specific about the exact time the skeletons were placed in the chamber, however given the information available it is highly likely that it occurred after 640CE and before 659CE.

The burial context reflects an expedient mortuary solution, in response to a rapid and overwhelming death toll. Investigations indicated no signs of violent trauma, and a demographic profile encompassing all ages and sexes, suggesting the assemblage coheres archaeologically with a sudden, nonviolent mortality event (Hendrix, 1995, 1998). The recent recovery of *Y. pestis* DNA from these remains (Adapa et al., 2025) now places the burial squarely within the arc of the First Pandemic (541–750 CE), offering the first genomic confirmation of plague in the Eastern Mediterranean from a securely dated archaeological context.

Jerash is particularly important to current pandemic scholarship, not just for the scale or suddenness of death, but the population profile revealed by the bioarchaeological methods. Stable isotope analysis offers a means to reconstruct birth origin and mobility, supporting investigations into whether individuals interred in the mass grave were local or had their origins in other regions, an important line of inquiry given Jerash's role as a trade and administrative hub (Watson, 2008). Mitochondrial DNA offers additional resolutions by enabling the reconstruction of maternal lineages, which can shed light on the ancestral diversity of individuals buried at the site.

3.4. Archaeological context: Jerash in comparison to other First-Pandemic burials

When viewed against the small and uneven corpus of archaeologically documented burials attributed to the First Pandemic, Jerash stands out as the only securely excavated, taphonomically verified mass grave in the Eastern Mediterranean that can be directly associated with *Y. pestis*. To situate Jerash within its broader archaeological landscape, it is useful to compare it with other sixth-to seventh-century burial contexts in the region.

At Gadara (Umm Qais) (Hübner and Weber, 1998), for example, the BD 30 crypt beneath the West Church contains a mixed assemblage of adult males and females, adolescents, and children, superficially recalling the broad demographic representation seen at Jerash. However, the mortuary logic of the Gadara crypt differs fundamentally: it is an elite, architecturally formalized burial space within a basilica complex, receiving individuals gradually over time as part of an ordered, selective funerary program. It is not a mass grave. By contrast, the chambers of the Jerash hippodrome preserve densely layered, rapidly deposited human remains with minimal ritual structure and clear indicators of emergency disposal. The repurpose of sealed vaulted rooms, normally used for storage or industrial activity, signals a breakdown of routine civic functions and an urgent response to sudden mortality. While Gadara provides a valuable comparative assemblage, only Jerash meets archaeological criteria for a catastrophic, epidemic-driven interment, now additionally confirmed by genomic identification of *Y. pestis*.

Beyond Jordan, written sources from Constantinople, Antioch, and Egypt vividly describe mass mortality and the creation of communal pits during the Justinianic Plague (Clark, 2023, Sarris, 2002,2022, Bystrický, 2023). Yet decades of urban excavation have not produced any securely dated sixth-century mass burial that combines (1) catastrophic taphonomy and (2) direct biomolecular evidence of plague. Potential epidemic assemblages such as the Garage Lux burials in Alexandria show intriguing demographic patterns (Lequette et al., 2024) but lack genomic confirmation. As such, Jerash does not replicate a known category of First-Pandemic mass graves; rather, it fills a conspicuous gap between textual testimony and the archaeological record. It remains the only site in the Near East where dense, sudden, multi-age burial can be directly tied to the First Pandemic through DNA, providing the first fully authenticated, catastrophic plague mass grave of Late Antiquity and offering an essential reference point for evaluating other candidate epidemic contexts.

3.5. Archaeological context: comparison with Black Death plague pits

Although securely identified mass graves from the First Pandemic are exceptionally rare, catastrophic plague burials become far more archaeologically visible during the Second Pandemic (14th–18th centuries), when the Black Death and its later recurrences produced well-documented communal pits across medieval and early modern Europe (Green and Fancy, 2024; Green, 2022). These sites form the clearest and most extensively studied archaeological comparanda for epidemic-driven mortuary responses, providing a benchmark against which earlier contexts such as Jerash can be evaluated. In this sense, Jerash represents the earliest known catastrophic plague mass grave, preceding the Black Death tradition by roughly eight centuries, and therefore occupies a unique position in the long-term history of epidemic burial practices.

Jerash can be considered in relation to well-studied Black Death mass graves, which display the defining characteristics of catastrophic plague deposition: extremely rapid interment, minimal funerary structure, high body density, broad demographic representation, and genomic confirmation of *Y. pestis*. Sites such as East Smithfield in London exemplify this pattern (Dewitte, 2010), and in many respects Jerash mirrors it, making the hippodrome chambers the closest known Late Antique analogue to these later medieval plague pits.

A key distinction nonetheless emerges. Black Death mass graves generally contain resident urban populations whose isotopic signatures cluster tightly, reflecting demographic coherence within a single city. By contrast, the Jerash assemblage displays a markedly wider range of childhood water signatures (as shown in the next section), indicating that those buried in the hippodrome chambers did not share a single local hydrological origin. This pattern suggests the presence of potentially transient individuals at the moment of crisis, an isotopic

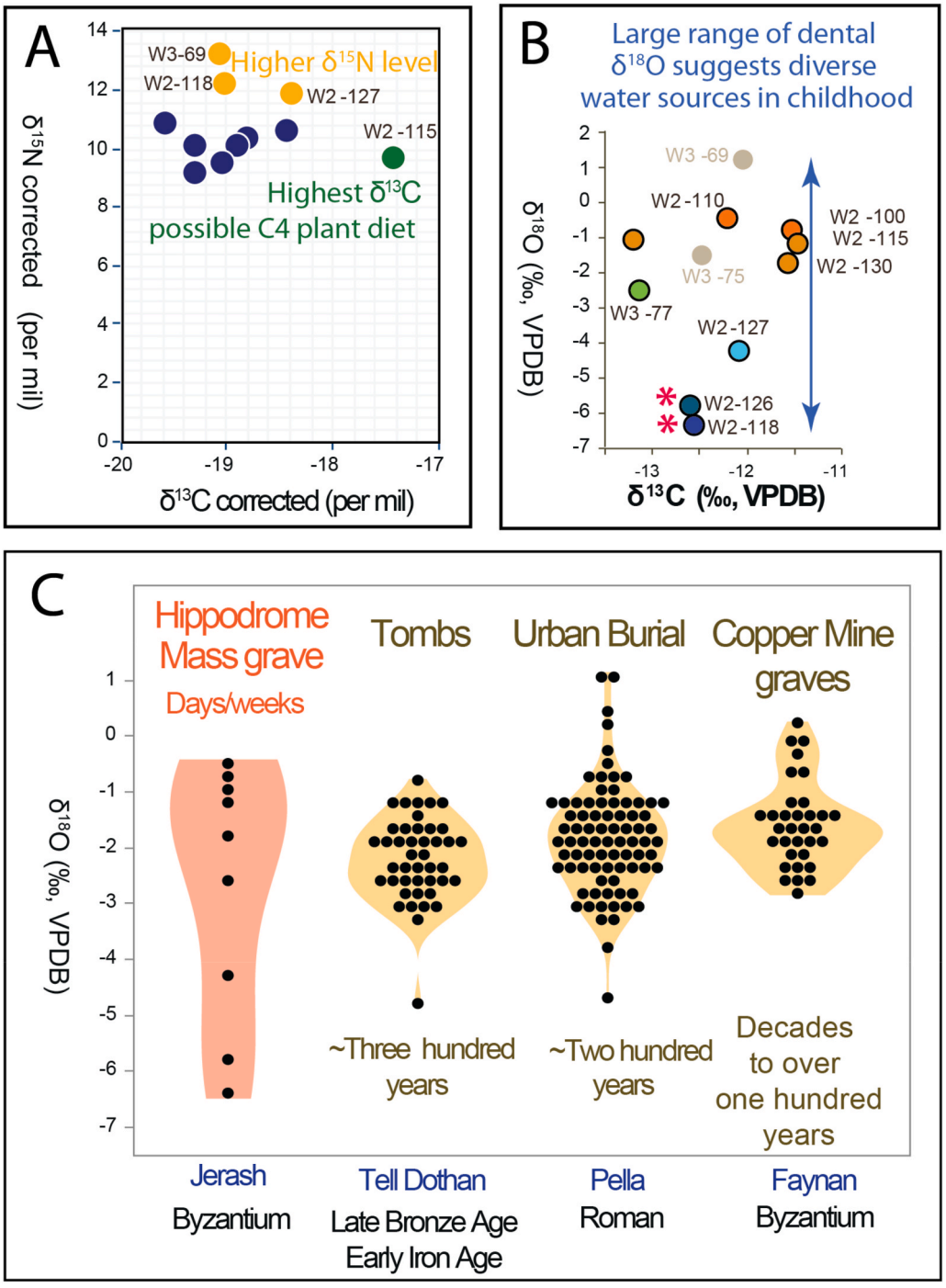

Fig. 2. Stable Isotope data of Individuals from the First Pandemic Mass Grave in Jerash A. Stable carbon and nitrogen isotope values from bone collagen reflect dietary patterns dominated by C_3 plants (*e.g.,* wheat, barley), with occasional C_4 contributions (*e.g.,* millet). Nitrogen isotope values show no evidence for sustained malnutrition or chronic metabolic stress among most individuals; only W3-69 may reflect acute physiological stress at or near the time of death. B. Oxygen isotope analysis of tooth enamel reveals considerable variation in $\delta^{18}O$ values, consistent with diverse childhood water source origins. The two grey dots indicate samples with lower quality readings and were excluded from analysis. Asterisks (*) indicate individuals with notably lower $\delta^{18}O$ values. These values likely reflect consumption of high-altitude water sources in childhood, either directly from upland areas or indirectly from highland-fed systems such as the upper Jordan River. C. Comparative $\delta^{18}O$ data from tooth enamel of Jerash (Byzantine), Tell Dothan (Late Bronze–Iron Age), Roman Pella, and the Byzantine copper-mining community at Faynan. Whereas these comparative cemeteries accumulated burials over centuries and exhibit narrower isotopic ranges characteristic of locally rooted populations, the Jerash mass grave, filled within days or weeks, shows a markedly wider spread of $\delta^{18}O$ values. This pattern in Jerash mass graves indicates highly heterogeneous childhood water sources and reflects the diverse lived experiences and geographic origins of the individuals buried during the First Pandemic.

heterogeneity not reported from medieval European plague pits. Thus, while Jerash and East Smithfield share the same taphonomic and epidemiological hallmarks of catastrophic mortality, the Jerash assemblage reflects a more socially and geographically diverse population, aligning with the dynamics of a provincial Byzantine city undergoing contraction and instability on the eve of the First Pandemic.

3.6. Stable isotope results indicate diverse life experiences of individuals

To explore the lived experiences and geographic backgrounds of the individuals interred in the mass grave, we next examine the stable isotope evidence (Supplemental Table S1). All Jerash collagen samples fall well within the accepted criteria for well-preserved archaeological collagen (molar C:N = 2.9–3.6). The Jerash values are tightly clustered (3.21–3.30), indicating excellent preservation, minimal diagenetic alteration, and reliability of $\delta^{13}C$ and $\delta^{15}N$ measurements.

Stable isotope analysis was conducted on 11 individuals from the Jerash site, following well-established preparation methods (Tykot, 2020). Collagen was extracted from tooth roots and apatite from tooth enamel for 10 individuals, and from bone for one individual. The sample included tooth root samples from 1 third molar, 1 central incisor and 8 s molars. These 8 s molars represented diet during formation (ca. 8–15 years). Thus, our stable isotope data uncovered the dietary patterns in childhood (enamel) to early adolescence life (collagen) stages of the victims.

Regarding the collagen, all samples had reliable yields and ratios of C and N. Except for individual W2-115 (green dot in Fig. 2A), the $\delta^{13}C$ range was narrow and averaged −19.0 ‰, suggesting dietary protein based on C3 plants (*e.g.* wheat, barley and oats) and animal consumptions. Individual W2-115, with a $\delta^{13}C$ value of −17.4, was consuming 10 %; of its protein diet from C4 plants such as millet. The $\delta^{15}N$ values for this individual W2-115 were the second lowest of all teeth, at 9.7 ‰, with the range for all 11 individuals from 9.1 to 13.2 ‰.

At least three individuals (yellow dots in Fig. 2A) exhibit elevated $\delta^{15}N$ values. These likely reflect a combination of arid environmental conditions and the use of manured crops, and may also include higher animal-protein intake in some cases. One individual (W3-69) shows a particularly high $\delta^{15}N$ value with otherwise typical C3-based $\delta^{13}C$, a pattern that is best interpreted as lying at the upper end of expected variation for arid, manured agricultural regimes rather than as direct evidence of short-term metabolic stress (Fig. 2A)

The tooth enamel $\delta^{13}C$ values, which represent the diet at the time of the tooth enamel formation (3–8 years), range from −13.2 to −11.5 ‰, suggesting that C4 plants were consumed in significant quantities early in life for several individuals, including individual W2-115 (Fig. 2B).

A wide range of tooth enamel $\delta^{18}O$ were found and varied from −6.4 to −0.5 ‰, suggesting a variety of childhood water sources for these individuals (Fig. 2B). Two of the three individuals with the highest $\delta^{15}N$ values in collagen (Fig. 2A) also had the most negative $\delta^{18}O$ values in enamel apatite (indicted by * in Fig. 2B). While such values are typically associated with cooler or higher-altitude regions, they may also reflect origins in areas downstream of highland-fed freshwater systems (*e.g.*, Jordan River, Sea of Galilee). The parsimonious interpretation is that these individuals consumed water from high-altitude sources, whether directly or via river systems, during childhood.

3.7. Isotope context: comparative isotope evidence of Jerash diversity in Levantine isotopic stasis

The Jerash $\delta^{13}C$ and $\delta^{15}N$ values fall within the expected range for Roman–Byzantine populations in Jordan, closely matching those documented at Petra (1st century. BCE - 1st century CE) (Perry et al., 2020) and Khirbet Qazone (1st-3rd century CE) (Walker, 2021) in the south of Jordan. This indicates broadly similar dietary regimes dominated by C3 plants and terrestrial animal protein.

However, the $\delta^{18}O$ data reveal a striking contrast between Jerash and other Levantine populations (Fig. 2B and C). Comparative datasets from Tell Dothan (Late Bronze–Iron Age)(Gregoricka and Sheridan, 2017), Roman Pella (Perry et al., 2020), and the Byzantine copper-mining community at Faynan (Perry et al., 2009) represent long-term residential burial populations accumulated over decades or centuries. Each displays characteristically narrow $\delta^{18}O$ ranges, reflecting stable childhood water-use patterns in largely sedentary communities. Regional studies of Jordanian isotopic baselines (Sandias, 2011; Al-Shorman et al., 2025a, 2025b) show long-term isotopic stasis across the southern Levant, with isotopic values remaining remarkably stable both geographically and over time. These findings indicate that short-term, within-lifetime mobility is seldom detectable in collagen isotope records for typical Levantine populations.

The Jerash mass grave, formed within days or weeks during the First Pandemic, shows dramatically elevated $\delta^{18}O$ variability, in stark contrast to comparative sites that accumulated burials gradually over decades or centuries. Jerash exhibits the widest isotopic spread of all assemblages (SD = 2.28 ‰; range = 5.9 ‰), exceeding the variation at Late Bronze Age/Early Iron Age Tell Dothan by almost 3-fold ($p < 0.001$), at Roman Pella by roughly 2-fold ($p \approx 0.02$), and at Byzantine Faynan by about 3-fold ($p < 0.001$).This contrast is especially striking given that even periods historically associated with population movement, such as the Late Bronze Age “Sea Peoples” horizon, or contexts involving forced labor and displacement, including Roman-era exploitation of workers at the Faynan copper mines, nonetheless produce narrow $\delta^{18}O$ ranges consistent with locally rooted childhood origins. The unusually broad $\delta^{18}O$ distribution at Jerash therefore indicates that the individuals interred in the mass grave derived from highly diverse childhood hydrological environments, a level of heterogeneity unmatched in any other Levantine cemetery population.

Jerash lies at the ecological intersection of the highlands, the Jordan Valley, and the eastern steppe, where altitude, rainfall, and water sources shift over relatively short distances. Although such environmental variability can generate modest local isotopic differences, the magnitude of $\delta^{18}O$ diversity observed in the Jerash assemblage far exceeds what can be attributed to local landscape heterogeneity alone. This conclusion is reinforced by comparisons with two key contemporary and methodologically consistent baselines: the Byzantine-period copper-mining community at Faynan, chronologically overlapping with Jerash yet exhibiting a narrow $\delta^{18}O$ range, and the Roman–Byzantine residential population at Pella, whose isotope values were produced by the same analytical laboratory (the USF Tykot lab) and likewise show more narrowly clustered $\delta^{18}O$ signatures characteristic of a locally born community over 200 years. Together, these contrasts underscore that the isotopic breadth at Jerash reflects genuinely diverse childhood hydrological environments rather than artefacts of regional ecology or laboratory procedures.

Against the background of long-term isotopic stasis in the Levant, the comparative isotope evidence from Jerash suggests that the mass grave contains individuals of mixed geographic origins, including some who were likely raised beyond the immediate hinterland. We emphasize that future strontium analyses will be required to test hypotheses of birthplace. This demographic diversity accords with Jerash's role as a Roman–Byzantine regional center embedded in trade, administrative, monastic, and agricultural networks. In the extraordinary circumstances of a rapidly formed crisis burial, this otherwise invisible heterogeneity becomes archaeologically legible.

3.8. Mitochondrial DNA reveals different maternal lineages among Jerash victims

Our recent ancient DNA analysis yielded high genomic coverage of *Y. pestis* from eight samples representing five individuals interred in the Jerash mass grave. Genetic analyses consistently confirmed that all *Y. pestis* genomes belonged to the strain associated with the First Pandemic (Adapa et al., 2025), despite being isolated from individuals

exhibiting distinct biological profiles.

While the bacterial genomes were identical, stable isotope data (presented above) support the interpretation of demographic heterogeneity among the victims. Variation in enamel isotope values reflects a range of childhood diets, indicating that some individuals grew up in several distinct climatic and hydrological regions.

To further examine the host population, we extracted and analyzed human mitochondrial DNA (mtDNA) from two individuals with the highest sequencing depth (ranging from 100 to 400 million reads) (Supplemental Table S2). Although Adapa et al. (2025) reported that the *Y. pestis* genomes recovered from both individuals were identical, indicating infection by the same bacterial strain during the First Pandemic, their mitochondrial DNA profiles revealed distinct maternal lineages (Fig. 3), showing genetic diversity within the host population. One individual (W2-130d) carried haplogroup L3e, a lineage found commonly in African populations. Multiple diagnostic SNPs defining haplogroup L3e were observed, including 769A > G, 10688A > G, and 14872C > T. L3e is believed to have originated in the southern Sudan region of Central Africa, or in what is now Mozambique approximately 45,000 years ago, during the Upper Paleolithic period. Today, it remains the most prevalent L3 subclade among the Bantu-speaking populations, and is commonly observed in African-descended populations in the Americas, including African Americans and Afro-Brazilians (Bandelt et al., 2001; Harich et al., 2010).

In contrast, the other individual (W2-131) carried haplogroup H13. We identified H-lineage–specific diagnostic variants, including 10398A > G and 15670C > T, which define haplogroup H and its associated subclades. H13 is a subclade of the widespread European H lineage, more commonly associated with Central and Eastern Europe. H13 also has significant representation in Anatolia and the Caucasus. Subclades such as H13c have been identified in ancient Mesolithic individuals from Georgia dating back 9700 years, while H13a2a and H13a2b are found among modern Armenian populations (Jones et al., 2015).

The co-occurrence of identical pathogen genomes and diverse host genetic profiles within a single mortuary context highlights Jerash's role as a socially and geographically diverse urban center during the First Pandemic, bringing together individuals from different origins who were nonetheless equally vulnerable to the same disease.

3.9. *Genetics context: Jerash mtDNA in relation to Near Eastern maternal diversity*

A comparative overview of mitochondrial DNA (mtDNA) diversity across Levantine, Anatolian, and North African populations shows that both West Eurasian and African maternal lineages appear at low but consistent frequencies throughout the region. This provides the appropriate framework for interpreting the Jerash results.

Genome-wide ancient DNA from the Middle–Late Bronze Age Levant demonstrates that regional populations formed a coherent ancestry through admixture between local Neolithic groups and migrants related to Chalcolithic Zagros and early Caucasus populations (Agranat-Tamir et al., 2020). This mixed "Canaanite" genetic structure persisted into the Roman and Byzantine periods and forms a major component of the genetic ancestry of modern Levantine populations.

Comparable Byzantine-era mtDNA data from Sagalassos (11th–13th c. AD) (Ottoni et al., 2016) reinforce this pattern. The population there exhibits a predominantly West Eurasian maternal profile dominated by haplogroups H, J, T, K, U, W, and N1, with high haplotype diversity and

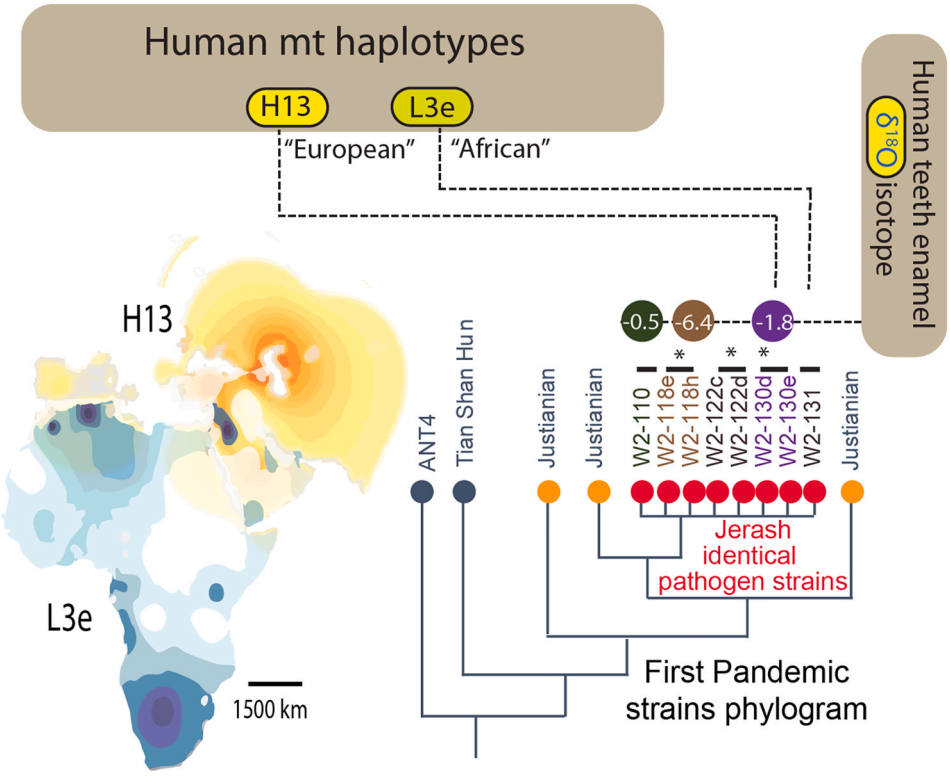

Fig. 3. Mitochondrial lineages of human hosts in Jerash Mass Grave
A schematic phylogram illustrates that whole-genome capture recovered the same *Yersinia pestis* strain from multiple individuals interred in the Jerash mass grave, as adapted from Adapa et al. (2025). Asterisks (*) denote two teeth sampled from the same individual. Stable isotope data from tooth enamel exhibit varied $\delta^{18}O$ and $\delta^{13}C$ values among individuals, indicating diverse childhood environments. Mitochondrial haplotypes identified in two individuals include L3e (blue gradient), a lineage prevalent in African populations, and H13 (yellow gradient), more common in Central and Eastern Europe. Darker shades on the map indicate regions with higher frequencies of the respective haplogroups, while lighter shades indicate lower frequencies. Mapping data were from Harich et al. (2010); Jones et al., 2015 [mt, mitochondrial]. (For interpretation of the references to colour in this figure legend, the reader is referred to the Web version of this article.)

affinities extending across Anatolia, Greece, Cyprus, the Levant, and Iran. African L-lineages are not present in the Sagalassos sample, but they are documented at low frequencies in the Eastern Mediterranean and Arabian Peninsula in both ancient and modern contexts.

Modern Jordanian mtDNA datasets (Zimmermann et al., 2019; González et al., 2008) show similar trends: Eurasian haplogroups (H, J, T, U, K) predominate, while African L-lineages occur at low to moderate frequencies. These frequencies indicate that African-associated maternal ancestry has long formed a minor but persistent component of regional genetic diversity.

Against this backdrop, the maternal haplogroups identified in the Jerash mass grave could fit within the known genetic diversity of the late antique Levant. Haplogroup H13 is a Eurasian lineage widely attested in both ancient and modern Levantine populations (Jones et al., 2015). In contrast, L3e reflects African-related maternal ancestry that likely entered the region within the past few thousand years. Several historically documented routes could have facilitated its arrival by the early 7th century CE, including Red Sea commerce (Phillips, 1997), Nile–Sinai population movements (Sá et al., 2022), Aksum–Arabia connections (Phillips, 1997), Roman military auxiliary recruitment (Isaac, 1992), and the longstanding Roman and Byzantine slave trades (Harper, 2017).

These observations are not intended to reconstruct the full maternal population structure of Jerash. Rather, they situate the two observed haplogroups within broader, well-established patterns of Near Eastern genetic diversity and historical connectivity, illustrating how individuals of different ancestries could have been present in a short-lived mass-fatality event.

4. Discussion: Integrating archaeological, isotopic, and genetic evidence to address the plague impact controversies and the Levantine Mobility Paradox

This study engages directly with two major debates in Late Antique and Near Eastern scholarship: (1) the impact of the First Pandemic, where interpretations diverge sharply between minimalists who see limited demographic disruption and maximalists who argue for substantial mortality and social consequences; and (2) the Levantine Mobility Paradox, the long-standing contradiction between a genetically diverse region shaped by centuries of admixture and the striking isotopic immobility observed in most burial populations. By integrating archaeological context, stable isotope analysis, and ancient DNA from the Jerash mass grave, we provide new empirical footing for both debates, showing how a single catastrophic event can expose demographic dynamics that are otherwise archaeologically invisible.

4.1. Jerash as the first securely identified First-Pandemic mass burial

Taken together, the archaeological, isotopic, and genetic results provide the first fully integrated picture of the Jerash plague burial. Archaeologically, the W2 chambers preserve a catastrophic, rapidly deposited mass grave whose taphonomic pattern mirrors later medieval Black Death pits (Dewitte, 2010; Green and Fancy, 2024; Signoli, 2022), making Jerash the earliest securely identified First-Pandemic mass burial in the Eastern Mediterranean. Stable isotope analysis adds a biological dimension: while long-term Levantine cemetery populations exhibit narrow $\delta^{18}O$ profiles, the Jerash assemblage, formed within days or weeks, shows unprecedented isotopic heterogeneity, indicating markedly diverse childhood water ecologies among those who died in the epidemic. Ancient DNA further anchors this interpretation, confirming a single *Y. pestis* outbreak (Adapa et al., 2025) and placing the victims within the expected maternal diversity of the Byzantine Levant.

Together, these lines of evidence reveal a population far more diverse in life histories than typical cemetery assemblages imply. The Jerash mass grave captures a moment when individuals shaped by different childhood environments, social circumstances, and lived trajectories were brought together in a single catastrophic event. This convergence, catastrophic taphonomy, heterogeneous isotopes, and genomic confirmation, provides an exceptional framework for reassessing population structure, vulnerability, and crisis response during the First Pandemic.

4.2. Jerash as a key data point in revisiting plague impact in Late Antiquity

The Jerash W2–W3 assemblage contributes directly to long-standing debates over the impact of the First Pandemic in the eastern Mediterranean. Current scholarship remains sharply divided between interpretations that view the Justinianic pandemic as a marginal event with limited societal consequences (Mordechai et al., 2019; Mordechai and Eisenberg, 2019), and those that argue for episodes of substantial mortality and disruption (Harper, 2017), *i.e.,* the minimalist vs. maximalist divide.

Minimalist readings, advanced most prominently by Eisenberg and others, maintain that even biomolecular detections of *Y. pestis* represent isolated instances, insufficient to demonstrate population-level crisis (Haldon, 2016; Mordechai and Eisenberg, 2019). In this framework, plague deaths are acknowledged but dismissed as anecdotal, with little interpretive weight for reconstructing demographic or social change. The Jerash mass grave provides the first biomolecularly confirmed, high-density mortuary context from a Late Antique city in the Levant, an empirical data point that exceeds the "single individual" paradigm on which minimalist interpretations rest. The rapid, unceremonious deposition of more than 200 individuals, stratigraphically associated with workshop debris, earthquake collapse, and early seventh-century ceramic production, demonstrates that plague fatalities could accumulate at scales necessitating extraordinary burial responses. This constitutes direct archaeological evidence for acute, localized mass mortality.

At the same time, the Jerash case also complicates maximalist narratives of societal collapse. The city continued to function, workshops resumed activity, and the urban fabric persisted into the Islamic period (Whitcomb, 1992; Walmsley, 2007). Jerash thus demonstrates that severe epidemic mortality and institutional continuity are not mutually exclusive outcomes.

From a public-health and epidemiological perspective, a pandemic is defined by large-scale geographic spread and population-level exposure to disease (Centers for Disease and Prevention, 2017; Organization, 2010), not by the collapse of political or economic institutions. Epidemic impact operates along at least two analytically distinct axes: (1) human toll, and (2) institutional or systemic shock. These dimensions are related but not equivalent and conflating them risks mischaracterizing the nature of past pandemics. As modern examples such as the 1918 influenza pandemic illustrate, extraordinarily lethal epidemics may occur without precipitating immediate economic or institutional collapse (Taubenberger and Morens, 2006).

Jerash therefore occupies a pivotal position in current debates. It provides a rare Late Antique mortuary signature of epidemic mass death while simultaneously demonstrating urban resilience and continuity. By anchoring human mortality within its archaeological and historical context, Jerash clarifies that the demographic reality of the First Pandemic cannot be assessed solely through macro-scale institutional proxies. Instead, human mortality remains the fundamental metric by which epidemic impact must be evaluated.

4.3. Current contradiction between long-term genetic admixture and isotopic stasis

Against the Jerash isotope and genetic background, we next turn to the apparent contradiction between long-term genomic admixture in the region (Agranat-Tamir et al., 2020; Jones et al., 2015) and the striking isotopic stasis observed in normal cemetery populations (Gregoricka and Sheridan, 2017; Perry et al., 2009; Al-Shorman et al., 2025a, 2025b). Jerash offers the first archaeological context capable of linking these two

scales of evidence.

Historically, the Levant is portrayed as a landscape of continual movement: the migrations and conflicts of the Late Bronze Age "Sea Peoples" (Cline, 2014; Sandars, 1985), biblical narratives of Exodus and return (Dever, 2003), Assyrian and Babylonian deportations (Na'Aman, 2005), Hellenistic colonization (McNicoll, 1993), and Roman–Byzantine military, administrative, and economic transfers across the Near East (Millar, 1993). These episodes dominate textual traditions and have shaped modern expectations of ancient population flux. Yet the archaeological and isotopic record tells a different story. Across the Bronze Age, Iron Age, Roman, and Byzantine periods, most people lived and died within stable local hydrological landscapes (Gregoricka and Sheridan, 2017; Perry et al., 2009; Al-Shorman et al., 2025a). For the majority, the lived experience was one of continuity rather than extensive, within-lifetime movement.

This tension, between the historical imagination of mobility and the measured isotopic stability of ordinary communities, provides the backdrop for what we term the Levantine Mobility Paradox.

4.4. The Levantine Mobility Paradox

The Levantine Mobility Paradox is the mismatch between a genetically mixed region and isotopically immobile individuals. Ancient DNA reveals the Levant as a long-term genomic mosaic shaped by millennia of admixture, whereas stable isotope studies consistently show that individuals in any given generation grew up and lived within stable, local hydrological landscapes.

These patterns are not contradictory: they reflect fundamentally different temporal resolutions. Genomic diversity captures slow, cumulative gene flow over centuries, while $\delta^{18}O$ values record childhood environments at the scale of individual lifetimes. Until now, however, no archaeological context has brought these two scales of evidence into direct dialogue.

4.5. Jerash as the missing link of Levantine population dynamics

Jerash could provide that missing link. The mass grave reveals that the population present during the epidemic was more heterogeneous in life histories than long-term cemetery baselines imply. Individual-level diversity existed in the region, but in typical burial assemblages it was demographically diluted and archaeologically invisible. The First Pandemic, through its sudden and catastrophic mortality, temporarily concentrated on this otherwise diffuse demographic layer. For the first time, variation in isotopic and genetic signatures becomes visible together.

In this sense, Jerash does not overturn the Levant's long-term isotopic stasis; it reveals where mobility was hiding. Individuals who died within days or weeks display more $\delta^{18}O$ variation than any known residential population in the region, yet their *Y. pestis* genomes confirm synchronous death. This combination exposes a demographic layer rarely captured in cemeteries: the steady trickle of economic migrants, itinerant laborers, climate-stressed families, pilgrims, soldiers, traders, and displaced persons (Bang, 2008; Isaac, 1992; Weiss, 2017; Horden and Purcell, 2000) whose movements were too diffuse to shift population-wide isotopic baselines but who cumulatively contributed to regional genetic diversity.

4.6. Potential resolution of the paradox

Thus, Jerash resolves the apparent puzzle: isotopic stasis reflects the residential majority, whereas genomic diversity reflects low-amplitude, long-term movement by transient and socially vulnerable groups. Modern anthropology and public-health research consistently shows that migration is driven from the margins (Castles et al., 2014; Massey et al., 1993), by economic precarity, warfare, climatic stress, and the search for labor or refuge, and not by the stable core of resident communities. Mobility in the ancient world was even more constrained and slower than today, meaning that the gradual inflow that shaped Levantine genetic diversity likely consisted of individuals moving under necessity rather than privilege.

A crisis event such as the First Pandemic temporarily concentrated these normally dispersed people into a single mortuary context, revealing forms of diversity that are otherwise archaeologically invisible. Jerash therefore provides the first empirical demonstration of how individual-level mobility and long-term admixture coexisted in Late Antiquity, and why only a catastrophic event can expose where mobility in antiquity was hiding.

4.7. Interdisciplinary synthesis

In synthesis, the archaeological, isotopic, and genetic evidence converge on a coherent interpretation. Jerash preserves the earliest catastrophic First-Pandemic plague mass grave in the Near East; its isotopes reveal unexpectedly diverse life histories; and its ancient DNA confirms both *Y. pestis* infection and maternal lineages typical of the Byzantine Levant. These findings provide a rare integrative view of how disease, urban density, and population diversity interacted in Late Antiquity. Continued strontium and genomic work will be necessary to refine this emerging portrait.

Taken together, Jerash demonstrates how a single crisis event can illuminate demographic realities that centuries of ordinary burial practices leave unseen.

CRediT authorship contribution statement

Karen Hendrix: Writing – review & editing, Writing – original draft, Resources, Investigation, Data curation, Conceptualization. **Swamy R. Adapa:** Project administration, Methodology, Investigation, Formal analysis. **Robert H. Tykot:** Writing – review & editing, Writing – original draft, Project administration, Methodology, Investigation, Formal analysis. **Gregory O'Corry-Crowe:** Writing – review & editing, Writing – original draft, Methodology. **Andrea Vianello:** Investigation. **Gloria C. Ferreira:** Writing – review & editing, Data curation. **Michael Decker:** Writing – original draft, Resources. **Rays H.Y. Jiang:** Writing – review & editing, Writing – original draft, Visualization, Supervision, Methodology, Investigation, Funding acquisition, Formal analysis, Data curation, Conceptualization.

Informed consent statement

Not applicable.

Institutional review board statement

Not applicable.

Jerash mass grave material

The human skeletal material was stored in the Archaeological Magazines in Jerash. The Department of Antiquities Jordan gave permission for the study and export of a small sample of the material in 1995/1998 and ethics approval is implicit with this approval to study. All Florida ethical protocols were followed for the samples under discussion in this study.

Funding

R.H.Y.J. received the USF Provost's CREATE Award (FY24–27), the USF COPH Research Award (FY23-25), and R.H.Y.J., R.H.T and A.V. received the USF Microbiome Institute Award (FY 24-25).

Declaration of competing interest

The authors declare no conflict of interest.

Acknowledgments

The authors would like to acknowledge the contribution by Dr Stephen Bourke, University of Sydney, Australia.

Appendix A. Supplementary data

Supplementary data to this article can be found online at https://doi.org/10.1016/j.jas.2026.106473.

Data availability

Data needed to evaluate the conclusions in the paper are available in the paper, Supplemental files, and the NCBI Sequence Read Archive (SRA) data archive.

References

Adapa, S.R., Hendrix, K., Upadhyay, A., Dutta, S., Vianello, A., O'Corry-Crowe, G., Ferrer, T., Monroy, J., Wood, E., Ferreira, G., Decker, M., Tripathy, S., Tykot, R., Jiang, R., 2025. Genetic evidence of Yersinia pestis from the first pandemic. Genes 16 (8), 926.

Agranat-Tamir, L., Waldman, S., Martin, M.A.S., Gokhman, D., Mishol, N., Eshel, T., Cheronet, O., Rohland, N., Mallick, S., Adamski, N., Lawson, A.M., Mah, M., Michel, M., Oppenheimer, J., Stewardson, K., Candilio, F., Keating, D., Gamarra, B., Tzur, S., Novak, M., Kalisher, R., Bechar, S., Eshed, V., Kennett, D.J., Faerman, M., Yahalom-Mack, N., Monge, J.M., Govrin, Y., Erel, Y., Yakir, B., Pinhasi, R., Carmi, S., Finkelstein, I., Carmel, L., Reich, D., 2020. The genomic history of the Bronze Age southern levant. Cell 181, 1146–1157.e11.

Al-Shorman, A., 2022. The Necropolis of Abila of the Decapolis 2019-2021. Archaeopress.

Al-Shorman, A., Perry, M., Coleman, D., 2025a. Ancient mobility in northern Jordan during the Roman and Byzantine periods using stable strontium isotope analysis of human dental enamel. J. Archaeol. Sci.: Reports 61, 104879.

Al-Shorman, A., Shqairat, M., Abudanah, F., Khwaileh, A., 2025b. Strontium isotope analysis of human dental enamel from a mass burial at Udhruh fortress, Southern Jordan: a paleomobility study. Bull. Int. Assoc. Paleodontol. 19, 16–24.

Bandelt, H.J., Alves-Silva, J., Guimarães, P.E., Santos, M.S., Brehm, A., Pereira, L., Coppa, A., Larruga, J.M., Rengo, C., Scozzari, R., Torroni, A., Prata, M.J., Amorim, A., Prado, V.F., Pena, S.D., 2001. Phylogeography of the human mitochondrial haplogroup L3e: a snapshot of African prehistory and Atlantic slave trade. Ann. Hum. Genet. 65, 549–563.

Bang, P.F., 2008. The Roman Bazaar: a Comparative Study of Trade and Markets in a Tributary Empire. Cambridge University Press, Cambridge.

Brock, S.P., 1976. Syriac sources for seventh-century plague. Byz. Z. 69, 3–20.

Buikstra, J.E., Ubelaker, D.H., 1994. Standards for data collection from human skeletal remains. Fayetteville, Arkansas Archeological Survey.

Bystrický, P., 2023. The Justinian Plague in literary sources. Forum Historiae 17 (1), 11–31.

Castles, S., De Haas, H., Miller, M.J., 2014. The Age of Migration: International Population Movements in the Modern World. Guilford Press, New York.

Centers For Disease, C. and Prevention, 2017. Pandemic Influenza. Centers for Disease Control and Prevention, Atlanta.

Clark, L.M., 2023. Burials of the Byzantine near East (4th–7th Centuries), vol. 2. Independent Scholarly Publication (Academia-hosted).

Cline, E.H., 2014. 1177 B.C.: the Year Civilization Collapsed. Princeton University Press, Princeton.

Conrad, L.I., 1981. The Plague in the Early Medieval near East. University of Oxford. Doctoral dissertation.

Conrad, L.I., 1994. Epidemic disease in central Syria in the late sixth century. In: LITTLE, L.K. (Ed.), Plague and the End of Antiquity. Cambridge University Press, Cambridge.

Dever, W.G., 2003. Who were the Early Israelites and Where did they Come From?, Grand Rapids, William B. Eerdmans Publishing Company.

Dewitte, S.N., 2010. Age patterns of mortality during the black death in London, A.D. 1349-1350. J. Archaeol. Sci. 37, 3394–3400.

Dols, M.W., 1974. Plague in early Islamic history. J. Am. Orient. Soc. 94, 371–383.

Eisenberg, M., Mordechai, L., 2020. The Justinianic plague and global pandemics: the making of the plague concept. Am. Hist. Rev. 125, 1632–1667.

González, A.M., Karadsheh, N., Maca-Meyer, N., Flores, C., Cabrera, V.M., Larruga, J.M., 2008. Mitochondrial DNA variation in Jordanians and their genetic relationship to other Middle East populations. Ann. Hum. Biol. 35, 212–231.

Green, M.H., 2022. A new definition of the black death: genetic findings and historical interpretations. De Medio Aevo 11, 139–155.

Green, M.H., Fancy, N., 2024. Plague history, Mongol history, and the processes of focalisation leading up to the Black Death: a response to Brack et al. Med. Hist. 68, 411–435.

Gregoricka, L.A., Sheridan, S.G., 2017. Continuity or conquest? A multi-isotope approach to investigating identity in the early Iron Age of the Southern Levant. Am. J. Phys. Anthropol. 162, 73–89.

Haldon, J., 2016. The Empire that would Not Die: the Paradox of Eastern Roman Survival, 640–740. Harvard University Press, Cambridge, MA.

Haldon, J., Stathakopoulos, D., 2018. The seventh-century plague revisited. Byzantine Mod. Greek Stud. 42, 156–175.

Harich, N., Costa, M.D., Fernandes, V., Kandil, M., Pereira, J.B., Silva, N.M., Pereira, L., 2010. The trans-saharan slave trade - clues from interpolation analyses and high-resolution characterization of mitochondrial DNA lineages. BMC Evol. Biol. 10, 138.

Harper, K., 2017. The Fate of Rome: Climate, Disease, and the End of an Empire. Princeton University Press, Princeton.

Hendrix, K., 1995. Preliminary investigation of the human skeletal remains from the hippodrome jarash. Annual of the Department of Antiquities Jordan XXXIX. Department of Antiquities, Jordan, pp. 560–562.

Hendrix, K., 1998. Further Investigations of the Human Skeletal Remains from the Hippodrome Jarash. Annual of the Department of Antiquities Jordan XLII, Department of Antiquities, Jordan, pp. 639–640.

Horden, P., Purcell, N., 2000. The Corrupting Sea: a Study of Mediterranean History. Oxford, Blackwell.

Hübner, U., Weber, T.M., 1998. Gadara 1998: the excavation of the five-aisled basilica at Umm qays: a preliminary report. Annu. Dep. Antiq. Jordan 42, 443–456.

Isaac, B., 1992. The Limits of Empire: the Roman Army in the East. Oxford University Press, Oxford.

Jones, E.R., Gonzalez-Fortes, G., Connell, S., Siska, V., Eriksson, A., Martiniano, R., Mclaughlin, R.L., Gallego Llorente, M., Cassidy, L.M., Gamba, C., Meshveliani, T., Bar-Yosef, O., Müller, W., Belfer-Cohen, A., Matskevich, Z., Jakeli, N., Higham, T.F. G., Currat, M., Lordkipanidze, D., Hofreiter, M., Manica, A., Pinhasi, R., Bradley, D. G., 2015. Upper Palaeolithic genomes reveal deep roots of modern Eurasians. Nat. Commun. 6, 8912.

Kehrberg, I., 2009. Byzantine ceramic productions and organisational aspects of sixth century AD pottery workshops at the hippodrome of jarash. Stud. Hist. Archaeol. Jordan 10, 493–512.

Kehrberg, I., 2016. Pottery and glass sherd-tools from Roman and Byzantine workshops at the Gerasa hippodrome and other sites. A reappraisal of earlier findings Studies in the History and Archaeology of Jordan (SHAJ) 12, 411–441.

Kehrberg, I., Ostrasz, A.A., 1994. Second report on mass burials in Cavea chambers W2 and W3 and the pottery dumps. Am. J. Archaeol. 98, 546–549.

Kehrberg, I., Ostrasz, A.A., 1997. A history of occupational changes at the site of the hippodrome of gerasa. In: ZAGHLOUL, M., AMR, K., ZAYADINE, F., NABEEL, R., TAWFIQ, N. (Eds.), Studies in the History and Archaeology of Jordan IV. Department of Antiquities of Jordan, Amman, pp. 167–173.

Kehrberg, I., Ostrasz, A.A., 2017. Ancient burials at the hippodrome of Gerasa/Jarash. Annu. Dep. Antiq. Jordan LVIII (181–213), 131–218.

Kennedy, D., 2013. Gerasa and the Decopolis. Bloomsbury Publishing.

Kennedy, H., 2007. Justinianic Plague in Syria and the archaeological evidence. Plague and the End of Antiquity: the Pandemic of 541-750. Little, L., pp. 87–98

Lequette, L., Sellier, P., Nenna, M.-D., Castex, D., 2024. Archaeological and biological evidence for the Justinianic plague: the "Garage Lux" in Alexandria? In: CASTEX, D., ROSSIGNOL, B. (Eds.), *Les Maladies Infectieuses Dans L'Antiquité*. UN@ Université Nouvelle-Aquitaine.

Lichtenberger, A., Raja, R., Seland, E.H., Simpson, I.A., 2021. Scaling up and zooming in: global history and high-definition archaeology perspectives on the longue durée of urban–environmental relations in Gerasa (Jerash, Jordan). J. Global Hist. 16, 395–414.

Little, L., 2007. Life and afterlife of the first Plague pandemic. In: Plague and the End of Antiquity: the Pandemic of, pp. 541–750.

Massey, D.S., Arango, J., Hugo, G., Kouaouci, A., Pellegrino, A., Taylor, J.E., 1993. Theories of international migration: a review and appraisal. Popul. Dev. Rev. 19, 431–466.

Mcdonald, B., 2024. The justinianic Plague and societal decline in the late Antique negev. In: JAMIESON, A., TULLY, C., HITCHCOCK, L. (Eds.), Plague in Antiquity. Ancient near Eastern Studies Supplement, vol. 65. Peeters, Leuven.

Mcnicoll, A.W., 1993. Hellenistic Fortifications from the Aegean to the Euphrates. Oxford University Press, Oxford.

Millar, F., 1993. The Roman near East, 31 BC–AD 337. Harvard University Press, Cambridge, MA.

Mordechai, L., Eisenberg, M., 2019. Rejecting Catastrophe: the Case of the Justinianic Plague*. Past & Present.

Mordechai, L., Eisenberg, M., Newfield, T.P., Izdebski, A., Kay, J.E., Poinar, H., 2019. The Justinianic Plague: an inconsequential pandemic? Proc. Natl. Acad. Sci. 116, 25546–25554.

Na'Aman, N., 2005. Ancient Israel and its Neighbors Interaction and Counteraction. Penn State University Press.

Organization, W.H., 2010. What is a Pandemic? World Health Organization, Geneva.

Ostrasz, A.A., 1989. The Hippodrome of gerasa: a report on excavations and research 1982–1987. In: Jerash Archaeological Project 1984–1988, vol. II. Department of Antiquities of Jordan, Amman.

Ostrasz, A.A., 1991. The Excavation and Restoration of the Hippodrome Jerash. A Synopsis. Annual of the Department of Antiquities Jordan XXXV Department of Antiquities, Jordan, pp. 237–250.

Ostrasz, A.A., 1993. Gerasa. Hippodrome. First report on burials in chamber W2. Am. J. Archaeol. 97, 498–500.

Ostrasz, A.A., Kehrberg-Ostrasz, I., 2020. The Hippodrome of Gerasa: a Provincial Roman Circus. Archaeopress Publishing, Oxford.
Ottoni, C., Rasteiro, R., Willet, R., Claeys, J., Talloen, P., Van De Vijver, K., Chikhi, L., Poblome, J., Decorte, R., 2016. Comparing maternal genetic variation across two millennia reveals the demographic history of an ancient human population in southwest Turkey. R. Soc. Open Sci. 3, 150250.
Perry, M.A., Coleman, D.S., Dettman, D.L., Al-Shiyab, A.H., 2009. An isotopic perspective on the transport of byzantine mining camp laborers into Southwestern Jordan. Am. J. Phys. Anthropol. 140, 429–441.
Perry, M.A., Provan, M., Tykot, R.H., Appleton, L.M., Lieurance, A.J., 2020. Using dental enamel to uncover the impact of childhood diet on mortality in Petra, Jordan. J. Archaeol. Sci.: Reports 29, 102181.
Phillips, J., 1997. Punt and aksum: Egypt and the horn of africa. J. Afr. Hist. 38, 423–457.
Rapp, C., 2023. Mobility and migration in Byzantium: who gets to tell the story? Early Mediev. Eur. 31, 360–379.
Russell, J.R., 1968. The Plague of shīrāwayh and the chronology of the sasanian Empire. J. Near E. Stud. 27, 296–307.
Sá, L., Almeida, M., Azonbakin, S., Matos, E., Franco-Duarte, R., Gómez-Carballa, A., Salas, A., Laleye, A., Rosa, A., Brehm, A., Richards, M.B., Soares, P., Rito, T., 2022. Phylogeography of sub-saharan mitochondrial lineages outside Africa highlights the roles of the Holocene climate changes and the Atlantic slave trade. Int. J. Mol. Sci. 23.
Sandars, N.K., 1985. The Sea Peoples: Warriors of the Ancient Mediterranean. Thames and Hudson, London.
Sandias, M., 2011. The Reconstruction of Diet and Environment in Ancient Jordan by Carbon and Nitrogen Stable Isotope Analysis of Human and Animal Remains. Cambridge University Press.
Sarris, P., 2002. The Justinianic plague: origins and effects. Continuity Change 17 (2), 169–182.
Sarris, P., 2022. New approaches to the 'Plague of Justinian'. Past Present 254, 315–346.
Taubenberger, J.K., Morens, D.M., 2006. 1918 influenza: the mother of all pandemics. Emerg. Infect. Dis. 12, 15–22.
Tykot, R.H., 2020. In: Smith, C. (Ed.), Bone Chemistry and Ancient Diet. Springer.
Walker, J., 2021. Social Identity and Life Course Stress in Nabataean Jordan. Unpublished Doctoral Dissertation, University of Pittsburgh USA.
Walmsley, A., 2007. Early Islamic Syria: an Archaeological Assessment. Duckworth, London.
Watson, P., 2008. The byzantine period. In: ADAMS, R. (Ed.), Jordan: an Archaeological Reader. Equinox, London.
Weiss, H., 2017. Megadrought and collapse. Oxford Research Encyclopedia of Climate Science. Oxford University Press, Oxford.
Whitcomb, D., 1992. Byzantine to early Islamic Jerash. J. Near E. Stud. 51, 101–120.
Zimmermann, B., Sturk-Andreaggi, K., Huber, N., Xavier, C., Saunier, J., Tahir, M., Chouery, E., Jalkh, N., Megarbane, A., Bodner, M., Coble, M., Irwin, J., Parsons, T., Parson, W., 2019. Mitochondrial DNA control region variation in Lebanon, Jordan, and Bahrain. Forensic Sci. Int.: Genetics 42, 99–102.